

QCD deconfinement transition line up to $\mu_B = 400$ MeV from finite volume lattice simulations

Szabolcs Borsányi¹, Zoltán Fodor^{1,2,3,4}, Jana N. Guenther¹, Paolo Parotto⁵, Attila Pásztor³, Ludovica Pirelli¹, Kálmán K. Szabó^{1,4}, and Chik Him Wong¹

¹Department of Physics, Wuppertal University, Gausstr. 20, D-42119, Wuppertal, Germany

²Pennsylvania State University, Department of Physics, State College, PA 16801, USA

³Institute for Theoretical Physics, ELTE Eötvös Loránd University, Pázmány P. sétány 1/A, H-1117 Budapest, Hungary

⁴Jülich Supercomputing Centre, Forschungszentrum Jülich, D-52425 Jülich, Germany

⁵Dipartimento di Fisica, Università di Torino and INFN Torino, Via P. Giuria 1, I-10125 Torino, Italy

Abstract. The QCD cross-over line in the temperature (T) – baryo-chemical potential (μ_B) plane has been computed by several lattice groups by calculating the chiral order parameter and its susceptibility at finite values of μ_B . In this work we focus on the deconfinement aspect of the transition between hadronic and Quark Gluon Plasma (QGP) phases. We define the deconfinement temperature as the peak position of the static quark entropy ($S_Q(T, \mu_B)$) in T , which is based on the renormalized Polyakov loop. We extrapolate $S_Q(T, \mu_B)$ based on high statistics finite temperature ensembles on a $16^3 \times 8$ lattice to finite density by means of a Taylor expansion to eighth order in μ_B (NNNLO) along the strangeness neutral line. For the simulations the 4HEX staggered action was used with 2+1 flavors at physical quark masses. In this setup the phase diagram can be drawn up to unprecedentedly high chemical potentials. Our results for the deconfinement temperature are in rough agreement with phenomenological estimates of the freeze-out curve in relativistic heavy ion collisions. In addition, we study the width of the deconfinement crossover. We show that up to $\mu_B \approx 400$ MeV, the deconfinement transition gets broader at higher densities, disfavoring the existence of a deconfinement critical endpoint in this range. Finally, we examine the transition line without the strangeness neutrality condition and observe a hint for the narrowing of the crossover towards large μ_B . This work is based on Ref. [1].

1 Introduction

In the last decades, a large body of evidence has been gathered on the crossover transition between the hadronic and Quark Gluon Plasma (QGP) phases of QCD at zero net baryon density, both from theory [2–7] and the phenomenology of heavy ion collision experiments [8–10]. Theoretically, there are two distinct aspects of the QCD transition. One is chiral symmetry restoration and the other is deconfinement. Lattice computations have mostly focused on chiral transitions compared with confinement aspects. The main goal of this work is to further study the deconfinement properties of the QCD medium at non-zero μ_B , by extending the accessible range in non-zero baryochemical potential.

Direct simulations at finite μ_B are hindered by the sign problem. Here we apply the Taylor method to the Polyakov loop and related observables using an eighth order expansion in the baryochemical potential-to-temperature ratio μ_B/T . We simulate lattices with a fixed number of time-slices, $N_t = 8$. The aspect ratio of $N_x/N_t = L \cdot T = 2$ is chosen in order to keep the sign problem under control, allowing us to reach 400 MeV in the baryo-chemical potential. We take advantage of the fact that the Polyakov loop is much less sensitive to finite volume corrections compared with chiral observables.[11] Simulating with extreme statistics (> 1 million configurations) at each temperature in a finite volume, we calculated the bare Polyakov loop in the entire range covered by the Beam Energy Scan program in collider mode.

The main observable calculated in this work is the static quark free energy F_Q , that is based on the expectation value P of the Polyakov loop: $P = \frac{1}{3} \frac{1}{V} \left\langle \sum_{\vec{x} \in V} \text{Tr} \prod_{t=0}^{N_t-1} U_0(t, \vec{x}) \right\rangle$. Here the product refers to the multiplication of the temporal link variables (U_0) of the gauge field along the entire temporal direction of the lattice that consists of N_t time slices. Thus, a Wilson line is formed and its normalized trace is the Polyakov loop. It is averaged over the three-volume V as well as over the ensemble of gauge configurations.

From P , the static quark free energy is then defined as $F_Q = -T \log P$. It follows from the additive nature of the F_Q renormalization that the static quark entropy $S_Q(T, \mu_B) = -\frac{\partial F_Q(T, \mu_B)}{\partial T}$ is well defined, and the scheme dependence cancels in the continuum limit. We defined the transition line as the peak of the renormalized static quark entropy.

2 Deconfinement versus Chiral transition lines

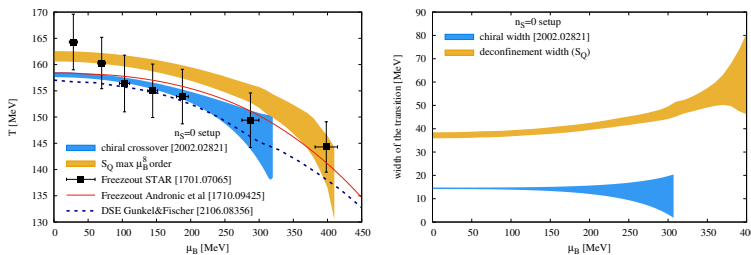


Figure 1. Left: the deconfinement line (orange) defined as the peak position of the static quark entropy (S_Q) at fixed μ_B as a function of μ_B . We add the chiral transition line from lattice QCD [12] in the phase diagram, defined from the peak of the full chiral susceptibility, as well as the corresponding result based on Dyson-Schwinger equations [13] (the latter used the $\mu_S = \mu_B/3$ scheme as an approximation to $n_S = 0$). We also include the chemical freeze-out parameters [14, 15]. Right: the width associated to the deconfinement (orange) and chiral (blue) transitions: the two differ already at $\mu_B = 0$. With increasing μ_B , while the chiral width is mostly constant, the deconfinement width grows.

The transition line in this work could be extended up to 400 MeV in the baryo-chemical potential. It closely follows the chiral crossover line, though the latter is known with larger errors and in a smaller range. With this result the phenomenological freeze-out line can be compared to the deconfinement line in a longer range than before. In particular, we cover the full range of the STAR freeze-out determination of Ref. [14]. The curvature of the static quark entropy at its peak can be used to define a width parameter for the deconfinement crossover. We showed that up to $\mu_B \approx 400$ MeV, the width parameter is getting larger at larger μ_B . This disfavors the existence of a deconfinement critical endpoint in this regime.

3 Comparison between $n_S = 0$ and $\mu_S = 0$

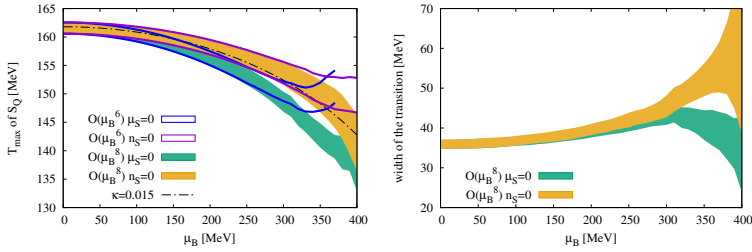


Figure 2. Left: The maximum position of $S_Q(T)$ for fixed baryo-chemical potential (μ_B). We show both setups with ($n_S = 0$) and without ($\mu_S = 0$) strangeness neutrality. We quote a rounded value of the curvature of the chiral transition and show the corresponding transition line for further guidance. We also show the sixth order result on the phase diagram. The eighth order is clearly significant above 350 MeV. Right: The width of the transition defined as $\Delta T(\mu_B) = \sqrt{-S_Q(T, \mu_B) \left| \frac{\partial^2 S_Q(T, \mu_B)}{\partial T^2} \right|_{T=T_c(\mu_B)}}$. While the width is similar for the strangeness neutral and in the $\mu_S = 0$ case we see a hint for a strengthening for $\mu_S = 0$ at the highest chemical potentials.

Finally, we compared the phenomenologically more relevant case of strangeness neutral matter ($n_S = 0$) with the theoretically more easily tractable case of zero strangeness chemical potential ($\mu_S = 0$). While the curvature of the $T_c(\mu_B)$ curve is slightly smaller for the strangeness neutral case, the width parameters are consistent (within error) up to $\mu_B \approx 300$ MeV. In the range $300 \text{ MeV} < \mu_B < 400$ MeV, there is a difference in the width parameters, with the $\mu_S = 0$ curve apparently turning around, and showing a narrowing of the transition (at least to this order in the Taylor expansion). This behavior might be caused by a critical endpoint beyond $\mu_B = 400$ MeV. One might speculate that such a narrowing can also happen to the $n_S = 0$ transition, but at higher values of μ_B . Unambiguously deciding whether this is the case calls for further investigations.

Acknowledgments

The project was supported by the BMBF Grant No. 05P21PXFCA. This work is also supported by the MKW NRW under the funding code NW21-024-A. Further funding was received from the DFG under the Project No. 496127839. This work was also supported by the Hungarian National Research, Development and Innovation Office, NKFIH Grant No. KKP126769. This work was also supported by the NKFIH excellence grant TKP2021_NKTA_64. This work is also supported by the Hungarian National Research, Development and Innovation Office under Project No. FK 14 7164. The authors gratefully acknowledge the Gauss Centre for Supercomputing e.V. (www.gauss-centre.eu) for funding this project by providing computing time on the GCS Supercomputer Juwels-Booster at Juelich Supercomputer Centre. We acknowledge the EuroHPC Joint Undertaking for awarding this project access to the EuroHPC supercomputer LUMI, hosted by CSC (Finland) and the LUMI consortium through a EuroHPC Extreme Access call.

References

- [1] S. Borsanyi, Z. Fodor, J.N. Guenther, P. Parotto, A. Pasztor, L. Pirelli, K.K. Szabo, C.H. Wong, QCD deconfinement transition line up to $\mu_B=400$ MeV from finite vol-

- ume lattice simulations, Phys. Rev. D **110**, 114507 (2024), 2410.06216. [10.1103/PhysRevD.110.114507](https://doi.org/10.1103/PhysRevD.110.114507)
- [2] Y. Aoki, G. Endrodi, Z. Fodor, S. Katz, K. Szabo, The Order of the quantum chromodynamics transition predicted by the standard model of particle physics, Nature **443**, 675 (2006), hep-lat/0611014. [10.1038/nature05120](https://doi.org/10.1038/nature05120)
- [3] S. Borsanyi et al. (Wuppertal-Budapest Collaboration), Is there still any T_c mystery in lattice QCD? Results with physical masses in the continuum limit III, JHEP **1009**, 073 (2010), 1005.3508. [10.1007/JHEP09\(2010\)073](https://doi.org/10.1007/JHEP09(2010)073)
- [4] H.T. Ding et al. (HotQCD), Chiral Phase Transition Temperature in (2+1)-Flavor QCD, Phys. Rev. Lett. **123**, 062002 (2019), 1903.04801. [10.1103/PhysRevLett.123.062002](https://doi.org/10.1103/PhysRevLett.123.062002)
- [5] A. Bazavov, T. Bhattacharya, M. Cheng, C. DeTar, H. Ding et al., The chiral and deconfinement aspects of the QCD transition, Phys.Rev. **D85**, 054503 (2012), 1111.1710. [10.1103/PhysRevD.85.054503](https://doi.org/10.1103/PhysRevD.85.054503)
- [6] A.Y. Kotov, M.P. Lombardo, A. Trunin, QCD transition at the physical point, and its scaling window from twisted mass Wilson fermions, Phys. Lett. B **823**, 136749 (2021), 2105.09842. [10.1016/j.physletb.2021.136749](https://doi.org/10.1016/j.physletb.2021.136749)
- [7] F. Cuteri, O. Philippen, A. Sciarra, On the order of the QCD chiral phase transition for different numbers of quark flavours, JHEP **11**, 141 (2021), 2107.12739. [10.1007/JHEP11\(2021\)141](https://doi.org/10.1007/JHEP11(2021)141)
- [8] S. Pratt, E. Sangaline, P. Sorensen, H. Wang, Constraining the Eq. of State of Super-Hadronic Matter from Heavy-Ion Collisions, Phys. Rev. Lett. **114**, 202301 (2015), 1501.04042. [10.1103/PhysRevLett.114.202301](https://doi.org/10.1103/PhysRevLett.114.202301)
- [9] L.G. Pang, K. Zhou, N. Su, H. Petersen, H. Stöcker, X.N. Wang, An equation-of-state-meter of quantum chromodynamics transition from deep learning, Nature Commun. **9**, 210 (2018), 1612.04262. [10.1038/s41467-017-02726-3](https://doi.org/10.1038/s41467-017-02726-3)
- [10] M. Abdallah et al. (STAR), Measurement of the Sixth-Order Cumulant of Net-Proton Multiplicity Distributions in Au+Au Collisions at $\sqrt{s_{NN}} = 27, 54.4, \text{ and } 200$ GeV at RHIC, Phys. Rev. Lett. **127**, 262301 (2021), 2105.14698. [10.1103/PhysRevLett.127.262301](https://doi.org/10.1103/PhysRevLett.127.262301)
- [11] S. Borsányi, Z. Fodor, J.N. Guenther, R. Kara, P. Parotto, A. Pásztor, L. Pirelli, C.H. Wong, Chiral versus deconfinement properties of the QCD crossover: Differences in the volume and chemical potential dependence from the lattice, Phys. Rev. D **111**, 014506 (2025). [10.1103/PhysRevD.111.014506](https://doi.org/10.1103/PhysRevD.111.014506)
- [12] S. Borsanyi, Z. Fodor, J.N. Guenther, R. Kara, S.D. Katz, P. Parotto, A. Pasztor, C. Ratti, K.K. Szabo, The QCD crossover at finite chemical potential from lattice simulations, Phys. Rev. Lett. **125**, 052001 (2020), 2002.02821.
- [13] P.J. Gunkel, C.S. Fischer, Locating the critical endpoint of QCD: Mesonic back-coupling effects, Phys. Rev. D **104**, 054022 (2021), 2106.08356. [10.1103/PhysRevD.104.054022](https://doi.org/10.1103/PhysRevD.104.054022)
- [14] L. Adamczyk et al. (STAR), Bulk Properties of the Medium Produced in Relativistic Heavy-Ion Collisions from the Beam Energy Scan Program, Phys. Rev. C **96**, 044904 (2017), 1701.07065. [10.1103/PhysRevC.96.044904](https://doi.org/10.1103/PhysRevC.96.044904)
- [15] A. Andronic, P. Braun-Munzinger, K. Redlich, J. Stachel, Decoding the phase structure of QCD via particle production at high energy, Nature **561**, 321 (2018), 1710.09425. [10.1038/s41586-018-0491-6](https://doi.org/10.1038/s41586-018-0491-6)